ADSORPTIVE, CATALYTIC AND ANTIMICROBIAL APPLICATIONS OF SERBIAN NATURAL CLINOPTILOLITE

N. Rajić[1], J. Milenković[2], J. Pavlović[2], S. Jevtić[1], I. Kaplanec[1], A. Rečnik[3], and J. Hrenović[4]

[1]*Faculty of Technology and Metallurgy, University of Belgrade, Karnegijeva 4, 11000 Belgrade, Serbia;*

[2]*Innovation Centre of the Faculty of Technology and Metallurgy, University of Belgrade, Karnegijeva 4, 11000 Belgrade, Serbia*

[3]*Institute Jozef Stefan, Jamova 39, 1000 Ljubljana, Slovenia*

[4]*Faculty of Science, Division of Biology, University of Zagreb, 10000 Zagreb, Croatia*

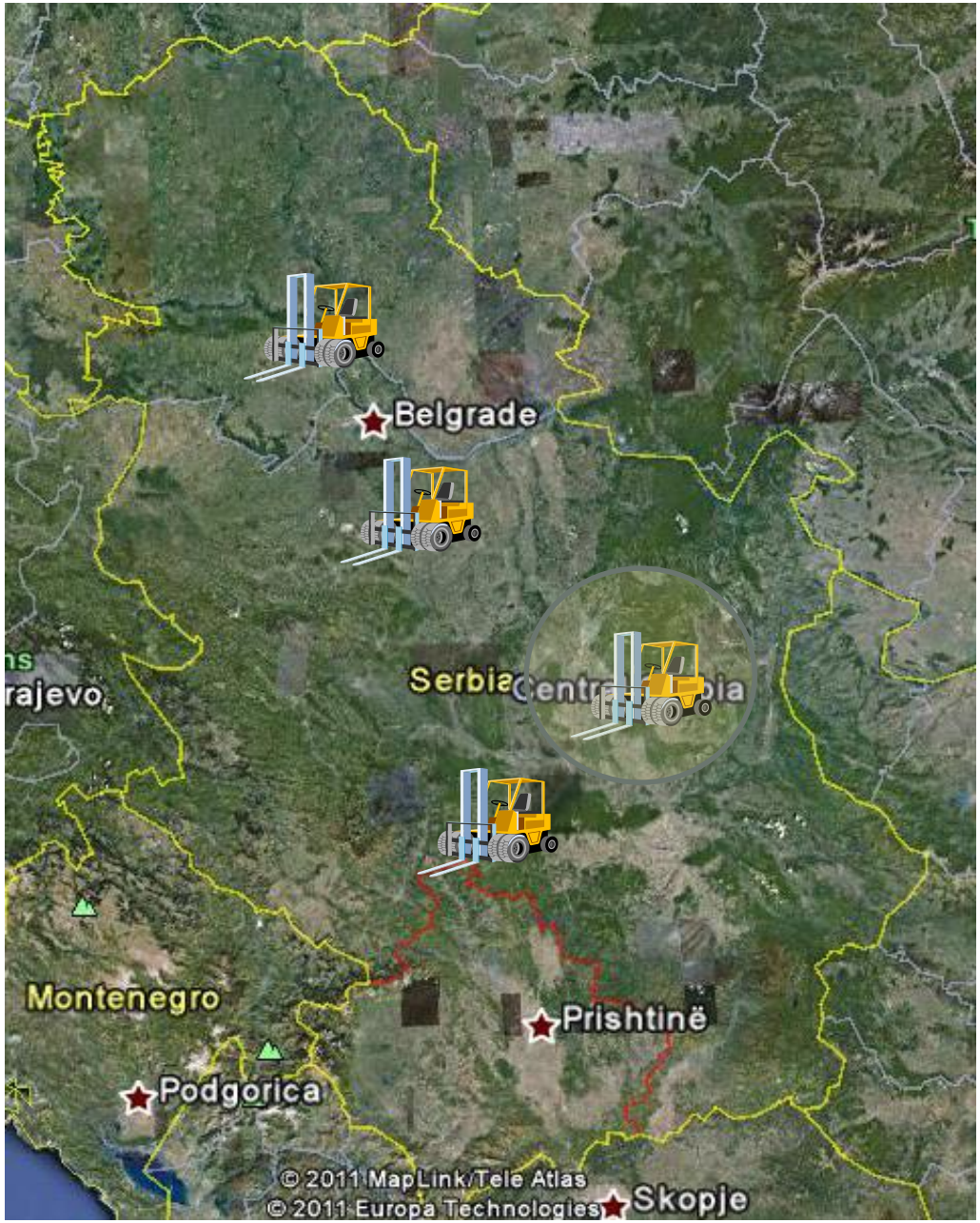

Zlatokop mine:
2.000.000 t

Study

- Adsorption
- Catalysis
- Antimicrobial action

Adsorption studies

Toxic cations

Water softening

Selected anions

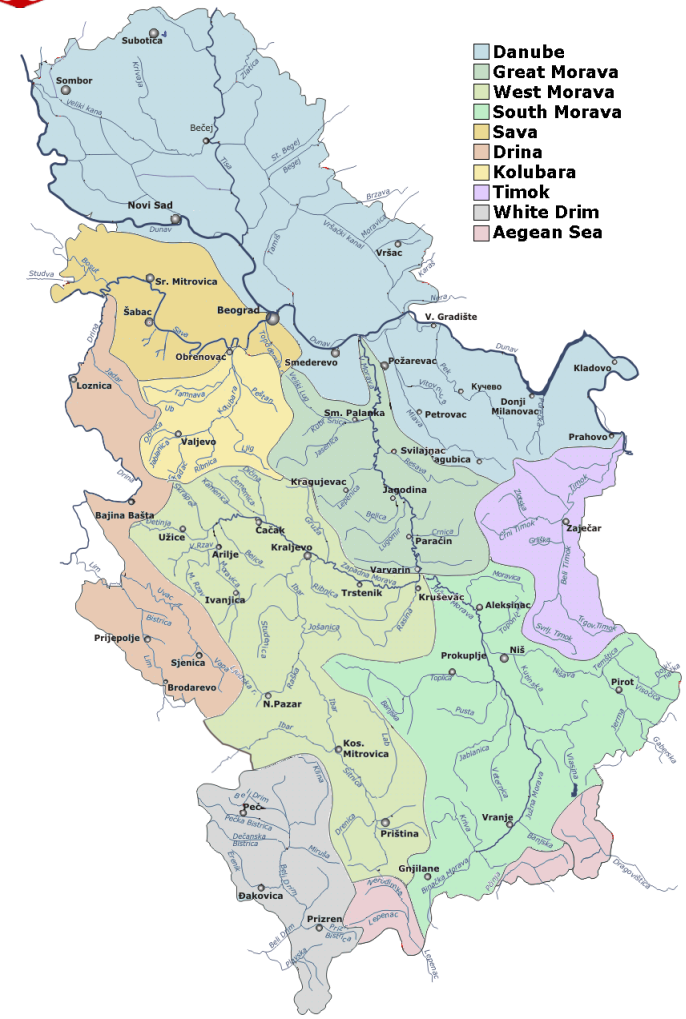

Serbia:

75 % of the population has access to modern water supply systems;

Quality of supplied water is not adequate in all regions.

Bor river – the most contaminated river in Europe


FLAMMIFER

- Clinoptilolite (75-85 wt.%)
- Feldspars (10-15 wt.%)
- Quartz (8-10 wt.%)

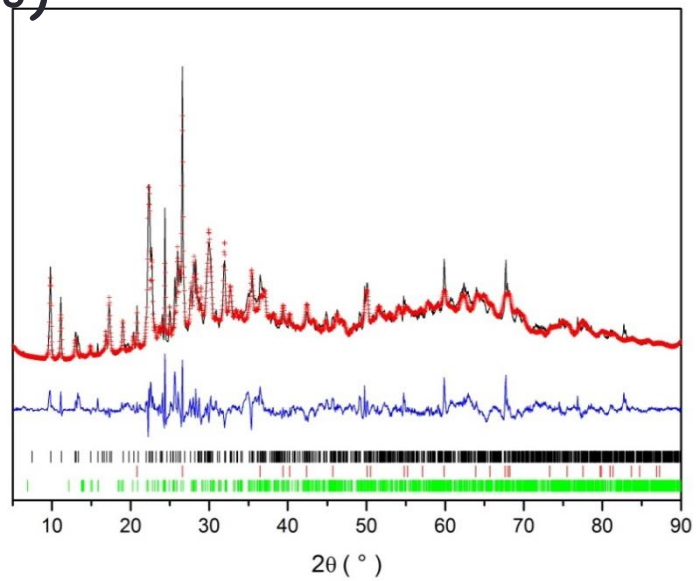

A quantitative XRPD analysis of the tuff sample

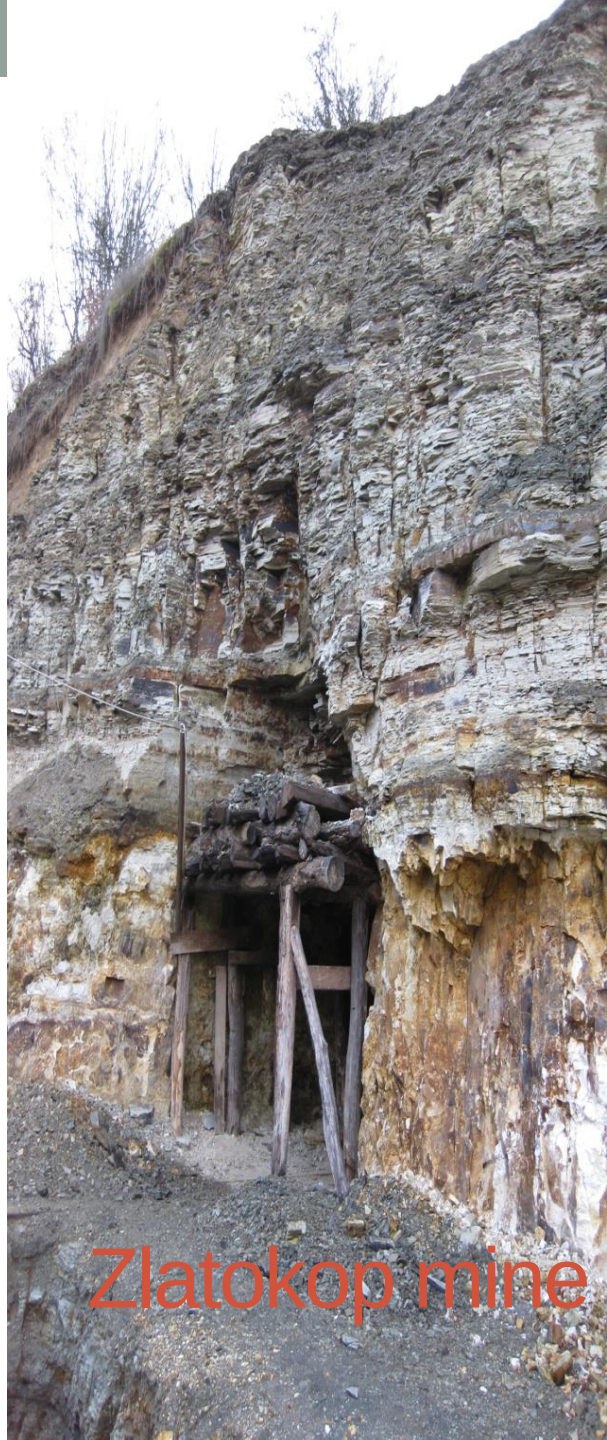

N. Rajic et al, J. Hazard Mater. 172 (2009) 1450-1457.

Mineral composition

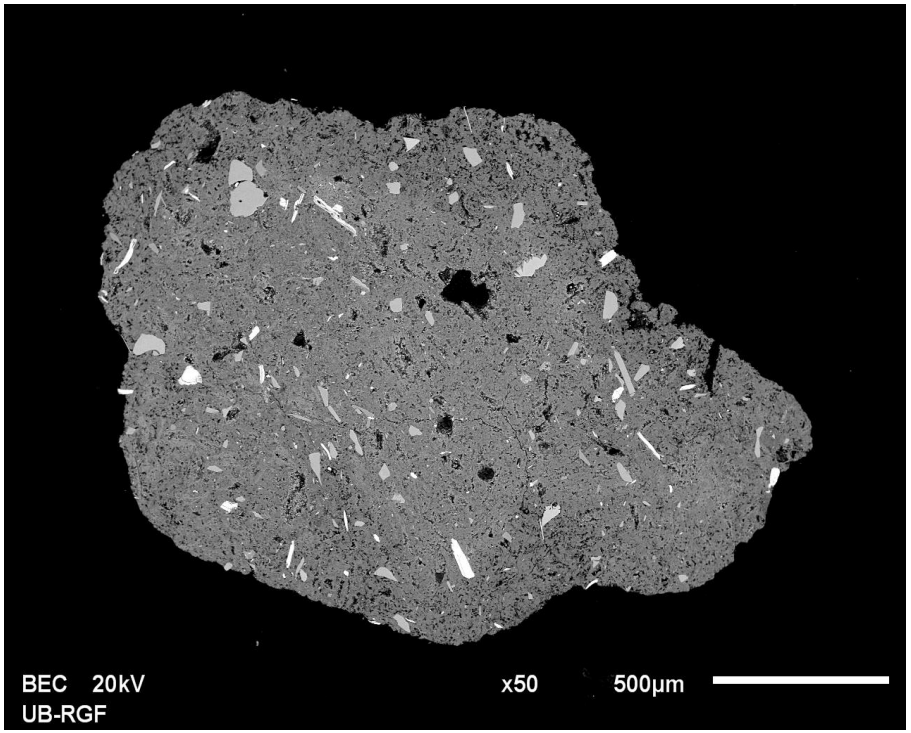

SEM photo of the tuff grain (different mineral phases differ in grey-scale brightness)

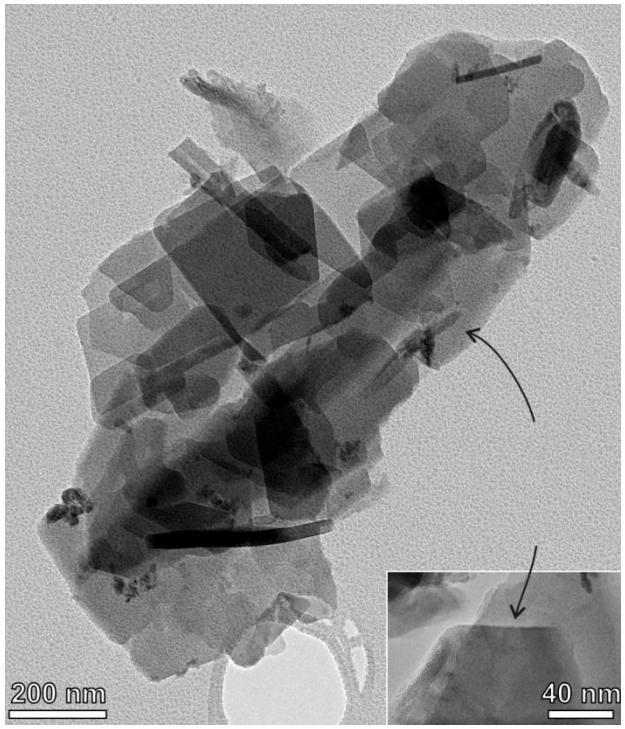

TEM image of the clinoptilolite phase

N. Rajic et al., J Phys Chem Solids 72 (2011) 800-803

Chemical composition

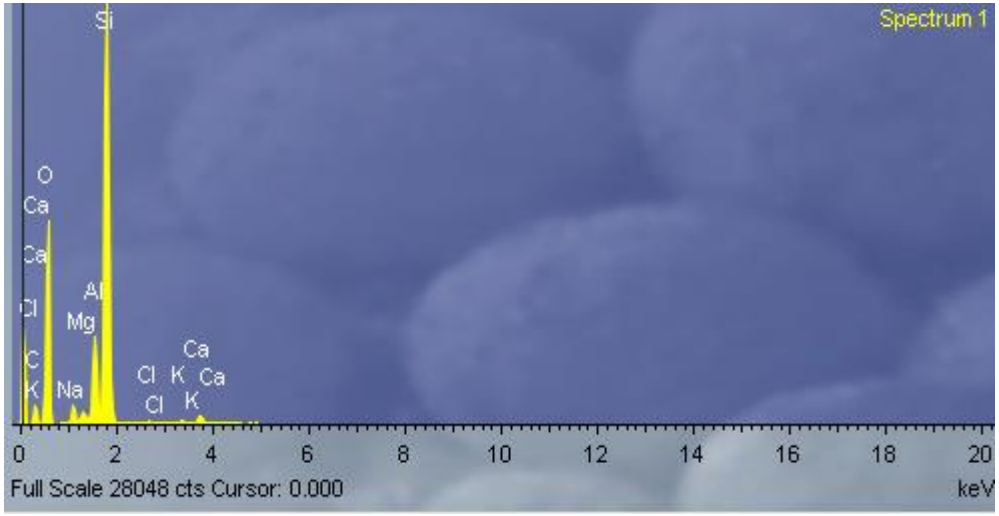

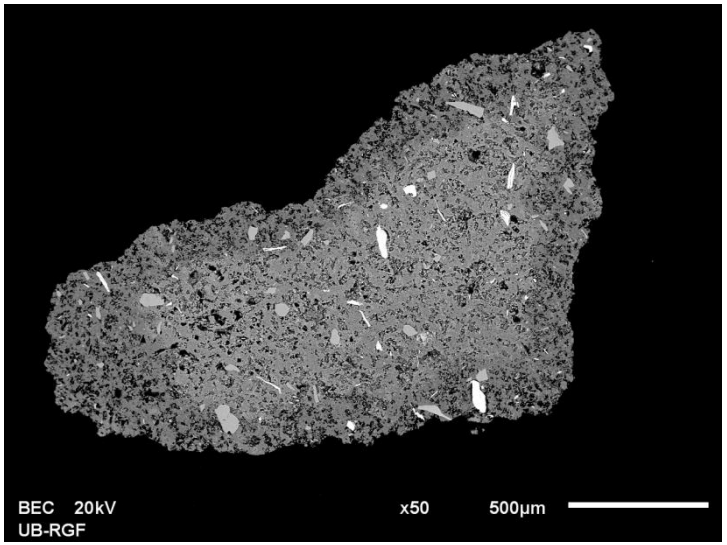

$$Ca_{1.6}Mg_{0.7}K_{0.7}Na_{0.3}Al_{5.5}Si_{26}O_{72}\cdot 23H_2O$$

N. Rajic et al, J. Hazard Mater. 172 (2009) 1450-1457.

Textural properties

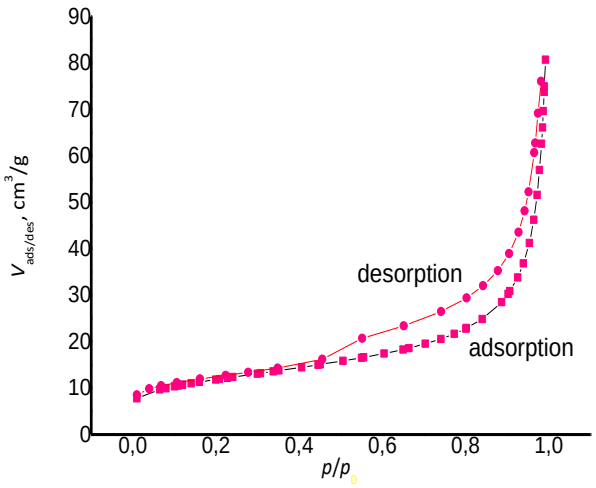

N_2 adsorption/desorption isotherms at -196 °C

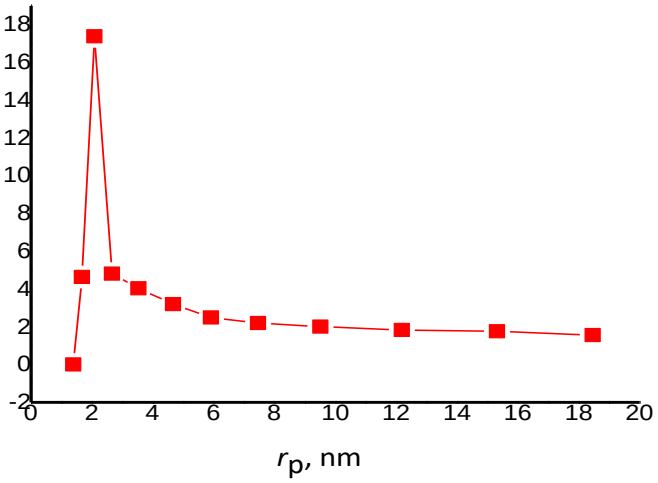

Pore size distribution

S_{BET}, $m^2\ g^{-1}$	42
S_{meso}, $m^2\ g^{-1}$	32
V_{mic}, $cm^3\ g^{-1}$	0.0052
A_L, $m^2\ g^{-1}$	57

S_{BET} – calculated BET method;
V_{mic}- micropore volume; S_{meso} - mesoporous surface area calculated using the αS-plot method; A_L - surface area from Langmuir method.

S Jevtić et al., Micropor Mesopor Mater 197 (2014) 92-100

Adsorption studies

Batch experiments

- Grain size: 0.063-0.1 mm
- Initial conc.:

  100-400 mg TM dm^{-3} (TM – Mn, Ni, Cu, Zn, Pb)
- Thermostatic bath:

  25-55 °C

- Adsorption isotherms
- Kinetic studies
  - kinetic models
  - diffusion effects
- Thermodynamic study

•N. Rajic et al., J. Hazardous Mat. 172 (2009) 1450-1454; N. Rajic et al, Appl. Surf. Sci. 257 (2010) 1524-1532; D. Stojakovic et al., J. Hazard Mat 185 (2011) 408-415; D. Stojakovic et al., Clay Clays Miner 59 (2011) 277-285; D. Stojakovic et al., Eniviron Eng Manag J 16 (2017) 131-140.

XPS analysis showed homogenous distribution of TM ions

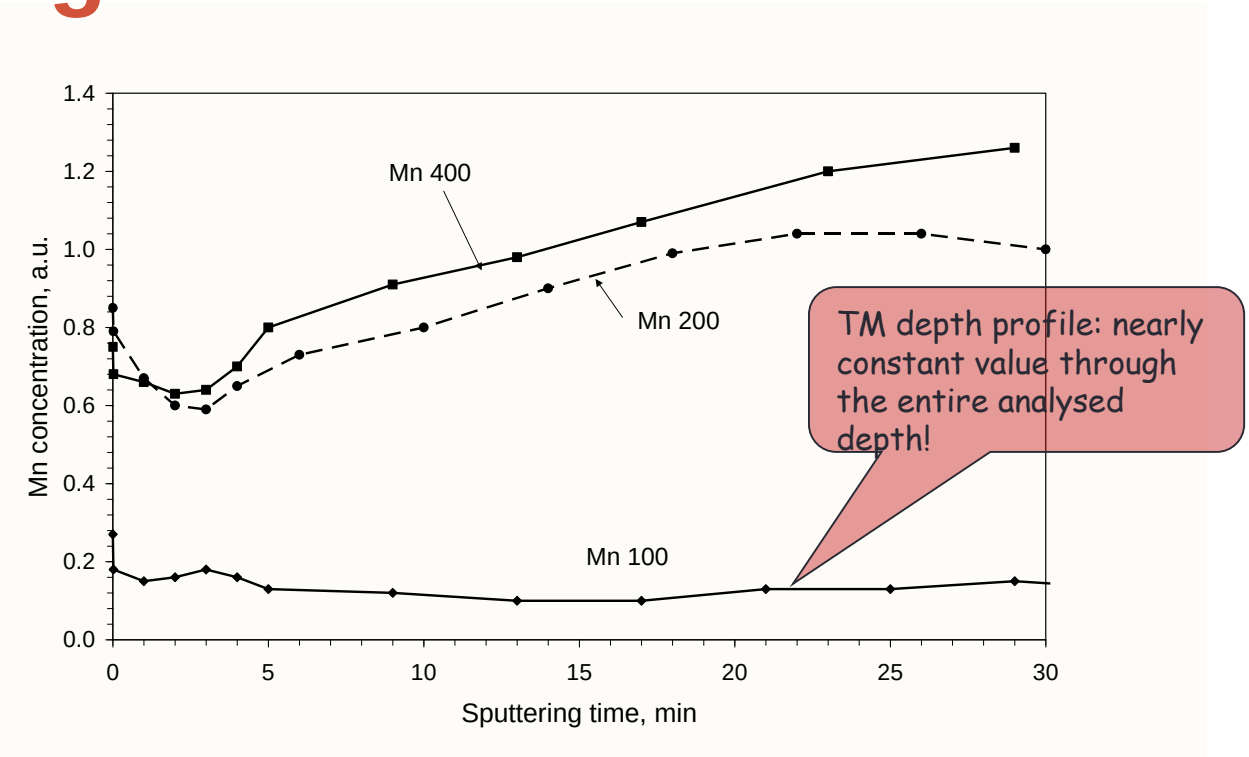

The Mn conc. as a function of the sputtering time obtained by XPS depth profiling on the samples with different Mn concentration

N. Rajic et al, J. Hazard Mater. 172 (2009) 1450-1457.

- Adsorption proceeds via an ion-exchange reaction following pseudo second-ordered kinetics.

- Cation type has a great impact on adsorption process. The equilibrium data for Pb and Zn were best described by Langmuir model, Sips model best fitted Mn and Ni and the isotherm for Cu was in accord with the Freundlich model;

- ΔG° decreases with temperature.

- ΔH° values of adsorption increasing in the series: $Pb^{2+} < Mn^{2+} < Zn^{2+} < Cu^{2+} < Ni^{2+}$.

- ΔS° values are positive, change following different trend of increase: $Mn^{2+} < Zn^{2+} < Pb^{2+} < Cu^{2+} < Ni^{2+}$

- **Removal rate increases in the series $Ni^{2+} < Mn^{2+} \approx Zn^{2+} < Cu^{2+} < Pb^{2+}$.**

Zeolitic tuff as a softener in improval of drinking water quality

Physico-chemical parameters of the spring water in the period 2006–2010.

Parameter	Conc. (mg/dm^3)	Max. permissible conc. (mg/dm^3)	Parameter	Conc, $\mu g/dm^3$	Max. permissible conc. ($\mu g/dm^3$)
pH	**9.5**	6.8-8.5	Mn	0.15	50
Turbidity	0.5 (NTU)	1.2 (NTU)	Fe	35	300
$KMnO_4$	8	8	Ni	0.4	20
Ca^{2+}	10	200	Cu	0.15	2000
Mg^{2+}	**90**	50	Zn	0.4	3000
SO_4^{2-}	7	250	As	0.22	10
NO_3^-	5	50	Se	0.26	10
NO_2^-	0.005	0.03	Mo	0.02	70
NH_4^+	0.2	0.1	Cd	0.003	3
PO_4^{3-}	0.02	0.003	Sb	0.01	3
B	2	300	Ba	0.41	700
Al	0.45	200	Hg	0.05	1
Cr	1.2	50	Pb	0.02	10

12,096 m^3/day (~ 120 inhabitants)

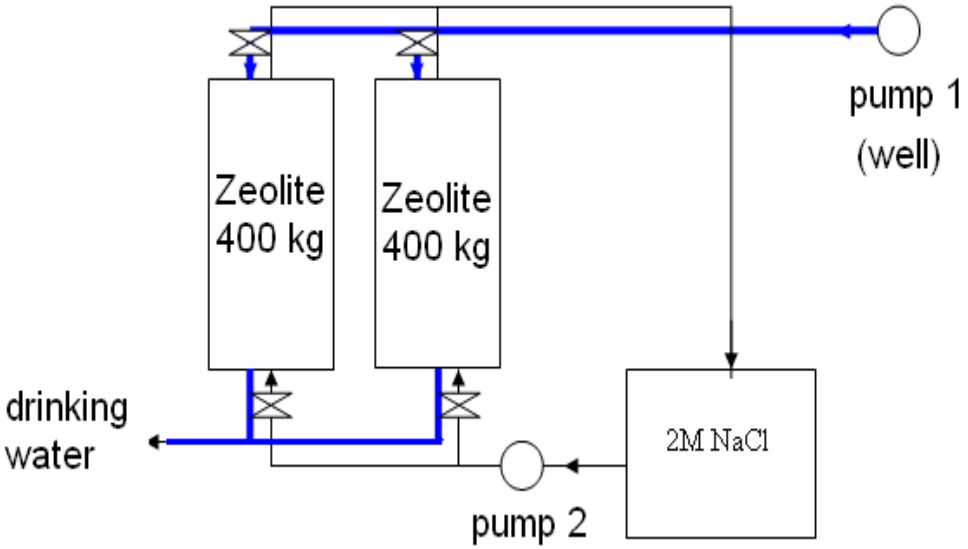

A pilot installed in 2013 in a small village near Raska. Small plant significantly decreased operational costs by replacing expensive synthetic polymer resins.

Removal of Mg and recovering of the saturated zeolite proceed intermittently.

S. Tomic et al, Clay Mineral, 47 (2012) 81-92

ADSORPTION OF SELECTED ANIONS

- selenite/selenate
- nitrite/nitrate
- phosphate
- salycilate

Modification of clinoptilolite

BC

Fe_2O_3

1. Modification with benzalkonium chloride (BC)

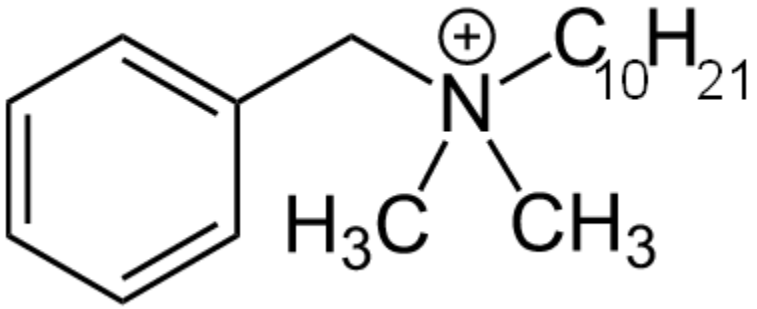

$Cl^{\ominus}$

BC

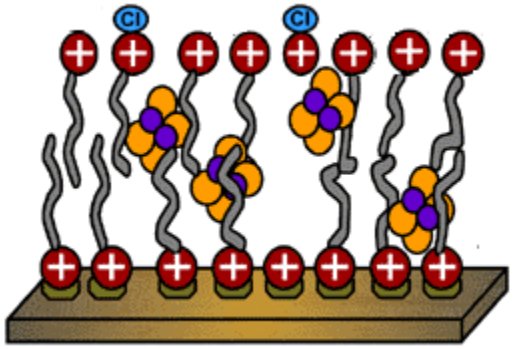

Cli surface modified with BC (BC does not enter channel system)

Adsorption of salycilate (SA) ions

- Pseudo second-ordered kinetics
- Removal rate ~ 80 % from SA solution with Co =100 μg per 1 cm^3)
- Relatively week electrostatic interactions between adsorbent and salycilate ions;
- Slowly realesing of adsorbed SA into phosphate buffer (pH~7)

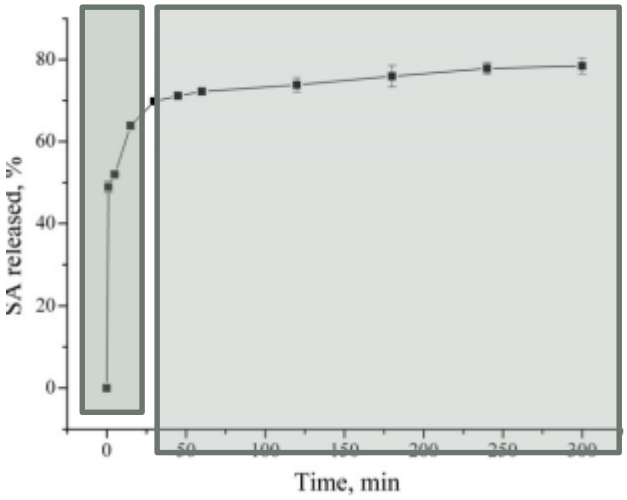

A two stage release:

50 % during first 15 min
30 % during 5 h

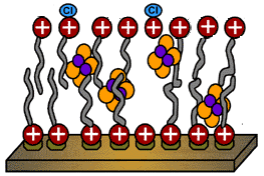

2. Modification with Fe_2O_3

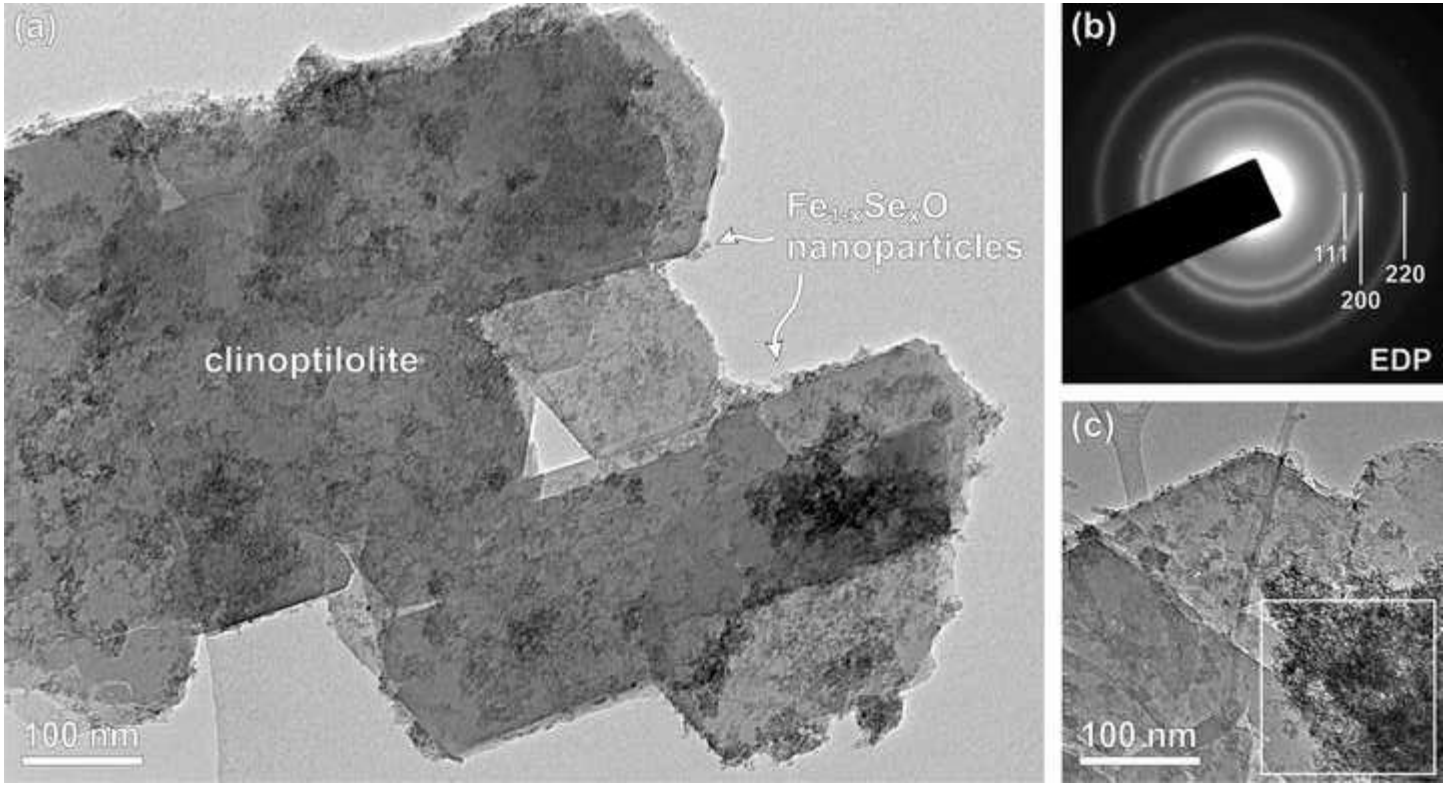

a) TEM images of the Se-containing adsorbent, b) Electron diffraction pattern (EDP) recorded from area marked (c).

Textural properties

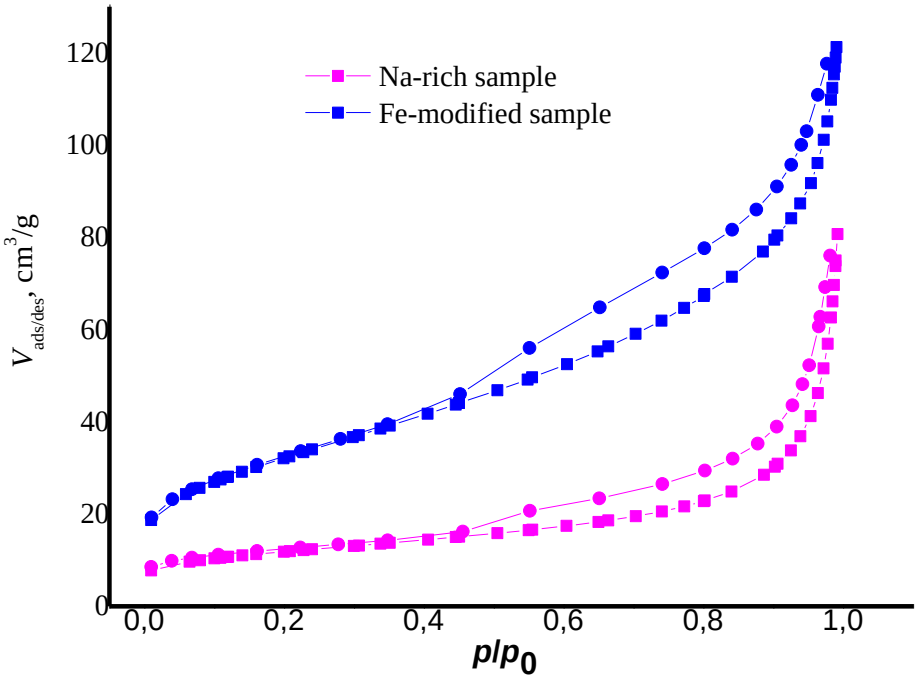

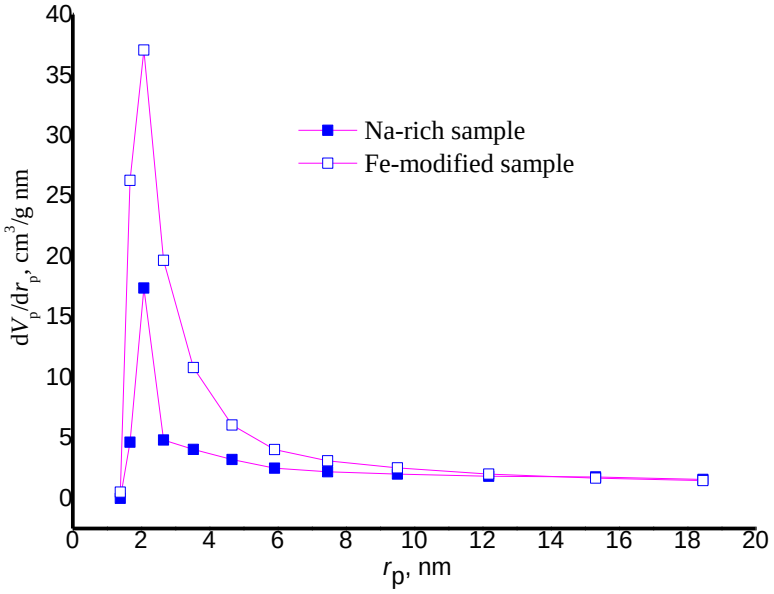

	S_{BET}	S_{meso}	A_L	V_{mic}
	$m^2\ g^{-1}$			$cm^3\ g^{-1}$
As-received	42	35	57	0.005
Fe-modified	117	71	161	0.039

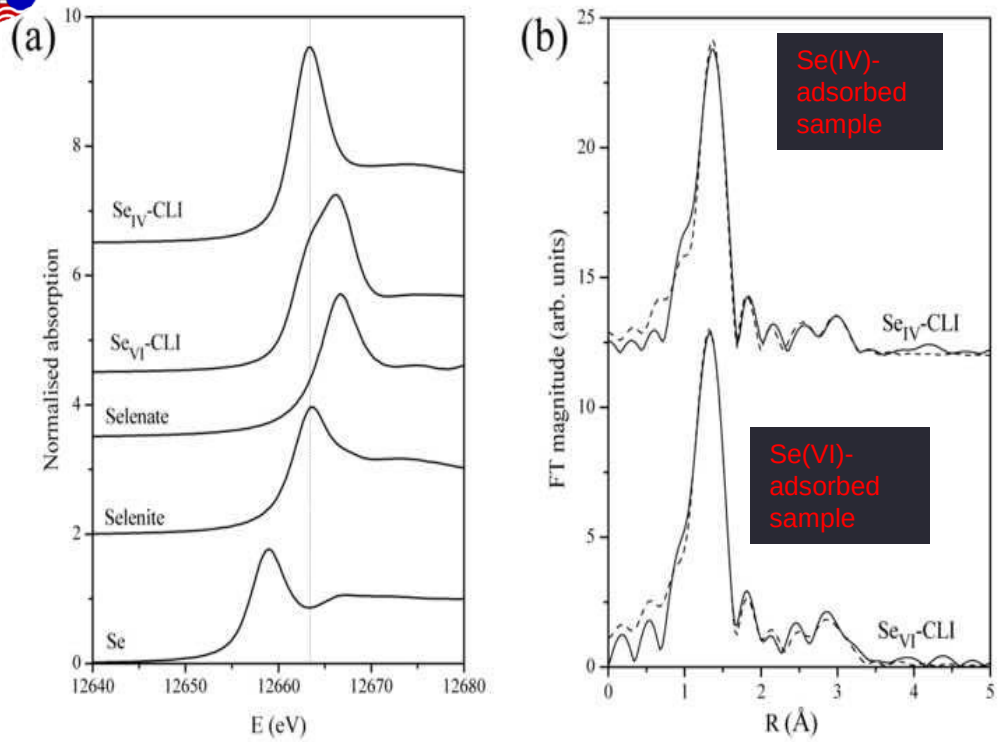

a) Se K-edge XANES of the adsorbents and the reference Se compounds

b) Fourier transforms of the k^3 -weighted Se K-edge EXAFS spectra solid line; best fit EXAFS model: dashed line)

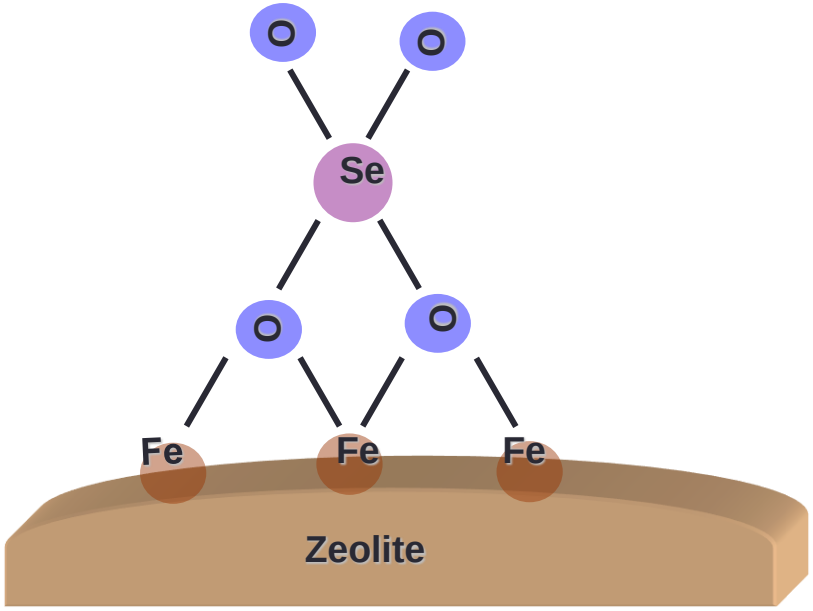

S Jevtić et al., Micropor Mesopor Mat 197 (2014) 92-100

Adsorption kinetics

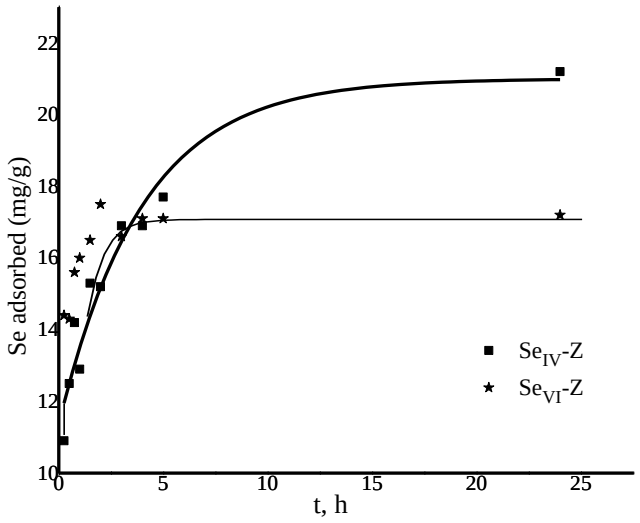

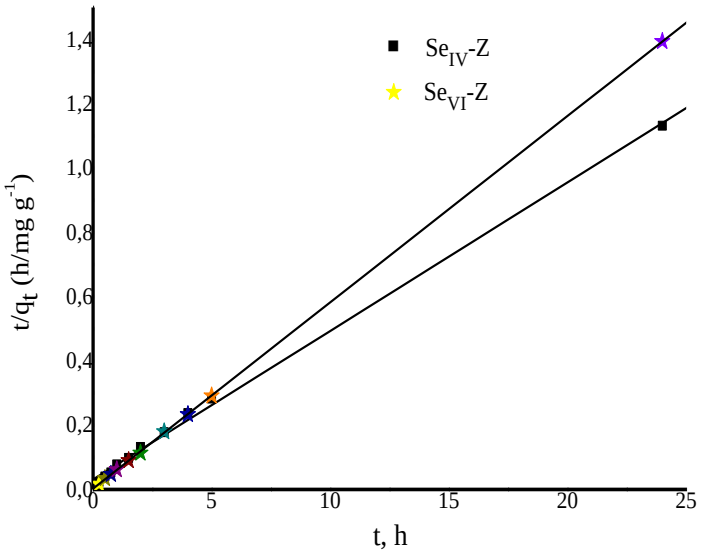

$$\frac{t}{q_t} = \frac{1}{k_2 q_e^2} + \frac{1}{q_e} t$$

Anion	q_e(mg g^{-1})	k [g mg^{-1} h^{-1}]	R^2
SeO_3^{2-}	21.6	0.0685	0.9991
SeO_4^{2-}	17.4	0.777	0.9999

S Jevtić et al., Micropor Mesopor Mater 197 (2014) 92-100

Phosphate adsorption

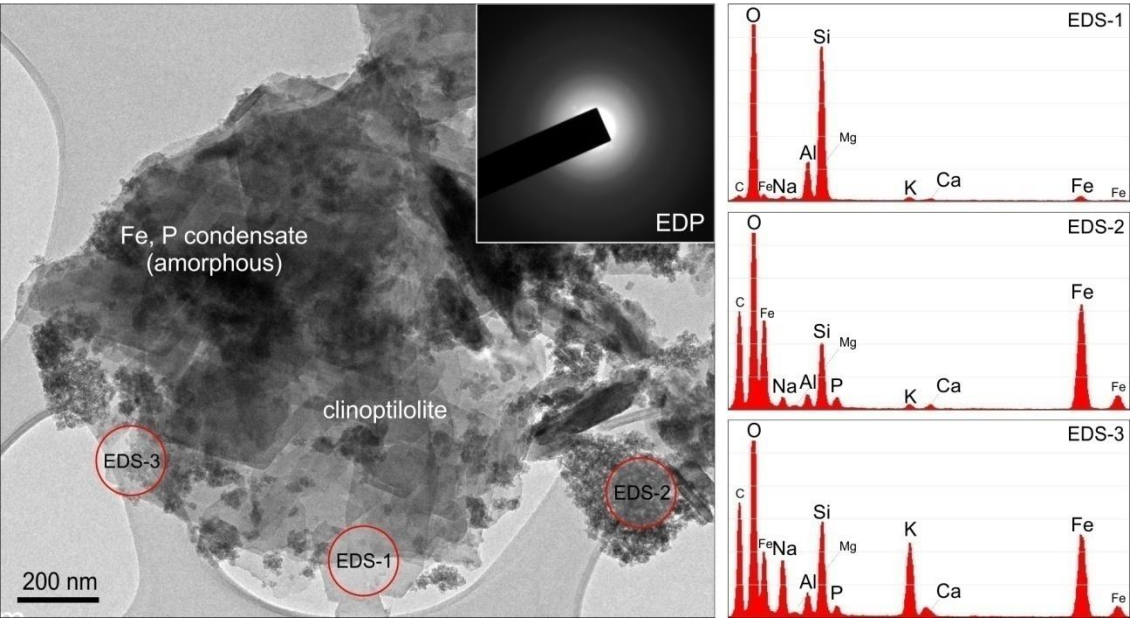

TEM image of phosphate-containing adsorbent. EDP (inset) indicates that the sample is amorphous. EDS analysis recorded from the areas indicated in the TEM image indicate an increase of the P-K peak with Fe-K stemming from the Fe-rich precipitate.

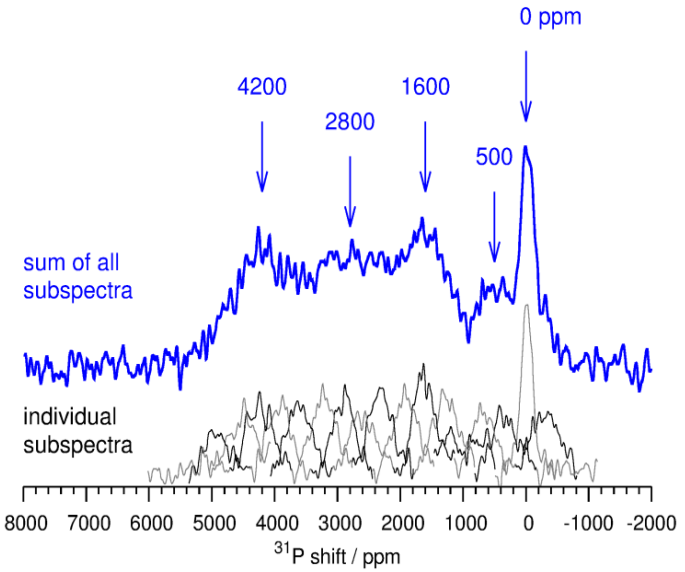

Spin-echo-mapping ^{31}P NMR spectrum of phosphate-containing adsorent.

I Kaplanec et al., Desalin. Water Treat. (2017), manuscript in publication.

Two types of interactions:
a) Electrostatic
b) Covalent (more pronounced).

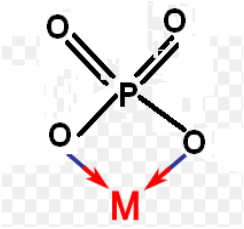

Adsorption kinetics of NO_3^-

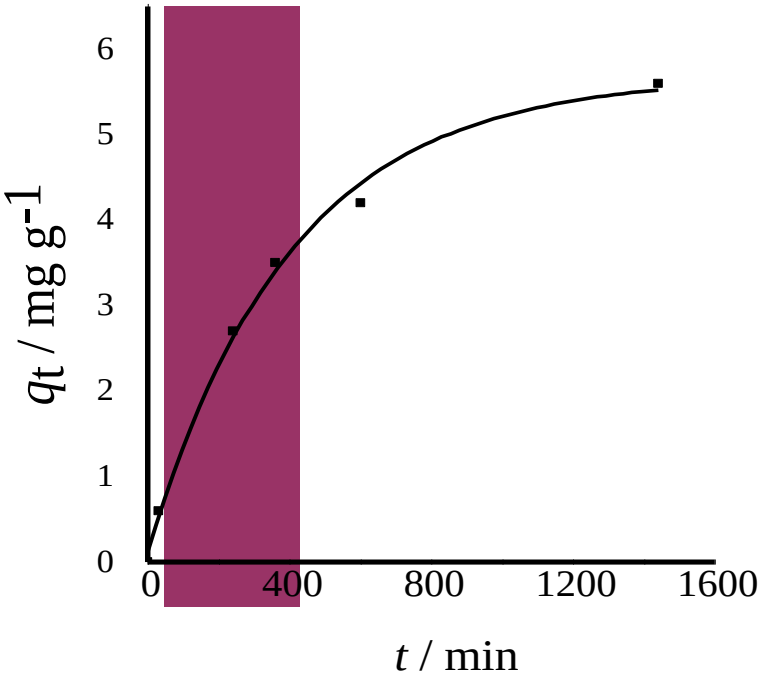

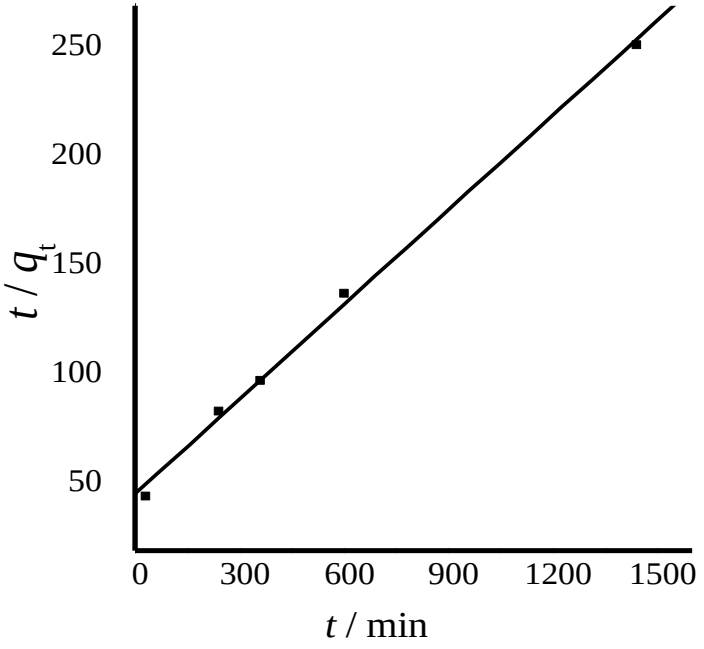

$$\frac{t}{q_t} = \frac{1}{k_2 q_e^2} + \frac{1}{q_e} t$$

Anion	q_e(mg g^{-1})	k [g mg^{-1} h^{-1}]	R^2
NO_3^-	6.91	0.0246	0.997

J. Pavlovic et al., J. Serb. Chem. Soc.79 (2014) 1-20

Catalysts prepared using zeolitic tuff

- Clinoptilolite as a matrix of nano-sized oxide particles;
  - catalytic activity in lignin pyrolysis
- Clinoptilolite as a support for super-acid particles
  - catalytic activity in esterification of LA

Clinoptilolite-based catalysts

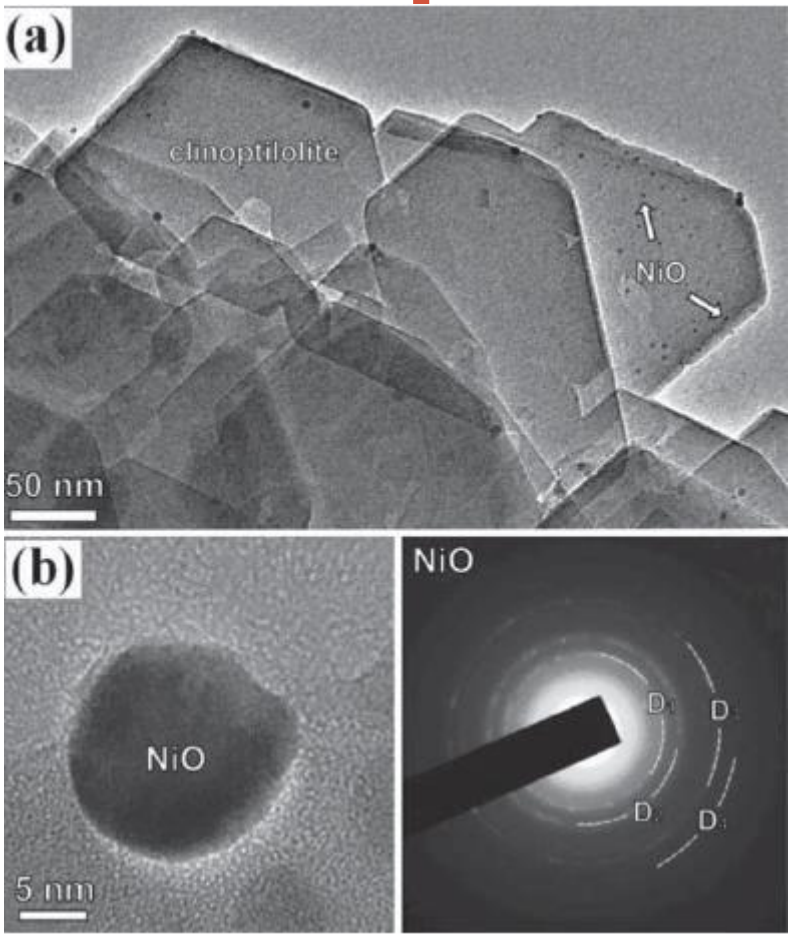

a) Transition metal-containing clinoptilolite can be converted into **catalytically active** material by calcination at 600 °C.

b) Well dispersed, fine nano-oxide particles formed by calcination.

c) **NiO, Cu_2O, ZnO**

N. Rajic et al, Appl. Surf. Sci. 257, (2010)1524-1532 ; N. Rajic et al, J. Phys. Chem Solids 72 (2011) 800-803

Formation of nano-oxide particles

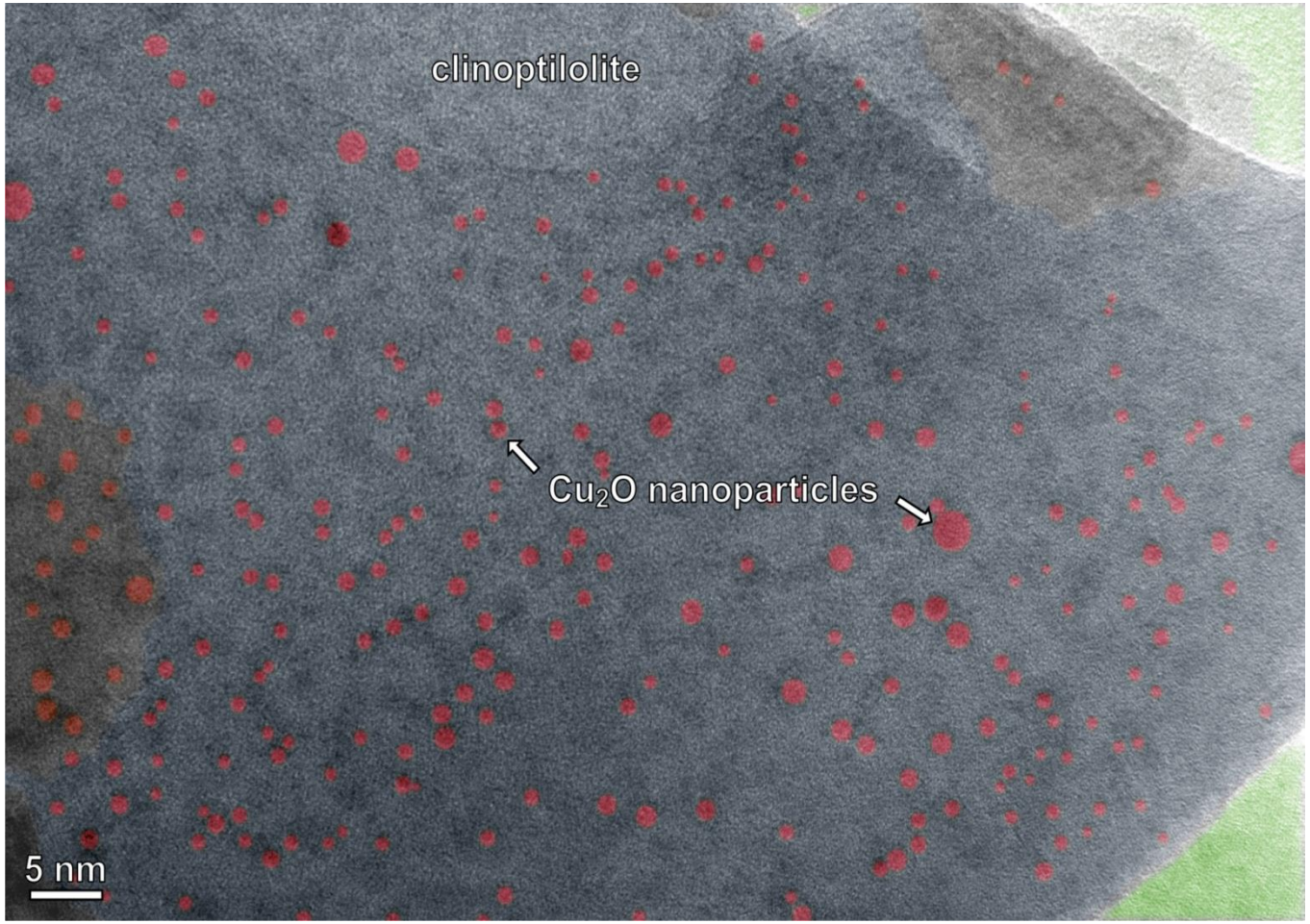

N. Rajic et al., J Phys Chem Solids 72 (2011) 800-803

Lignin pyrolisis

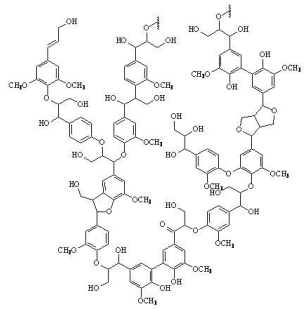

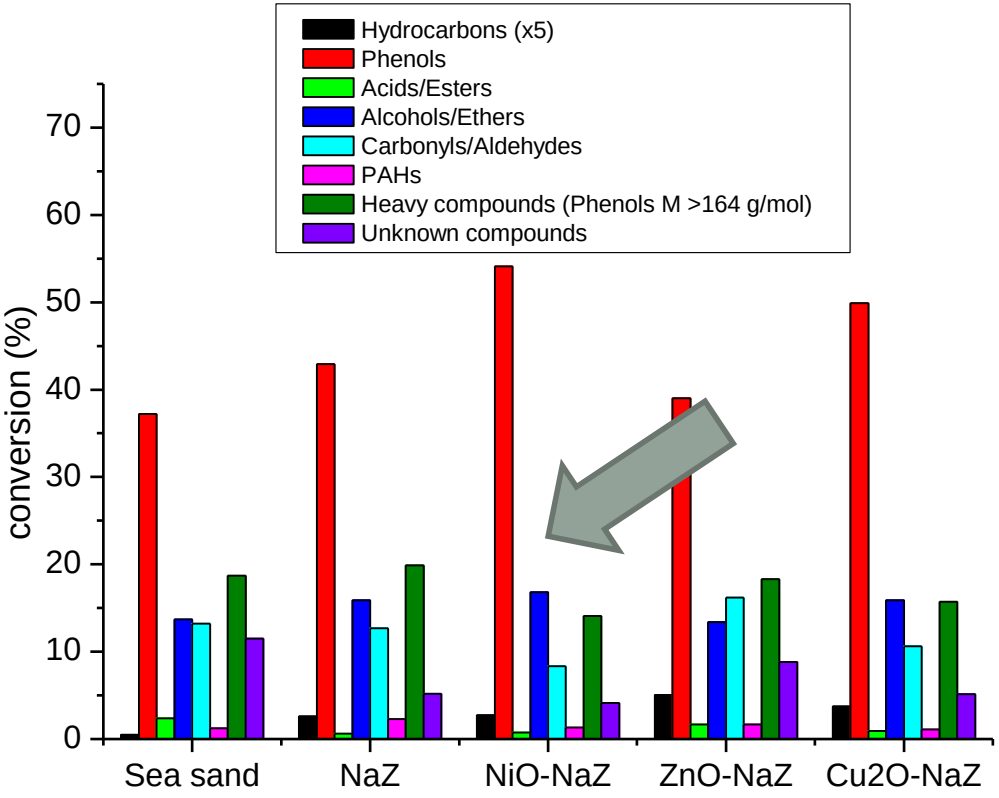

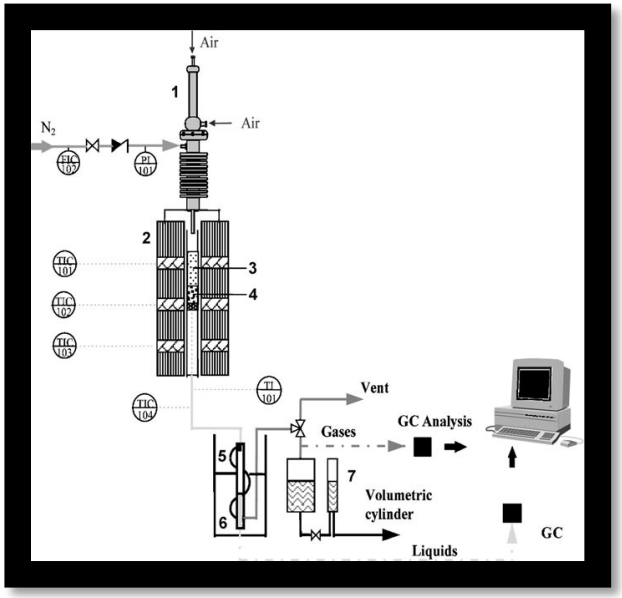

Catalytic test

Composition of the organic phase from the pyrolysis reaction.

N. Rajic et al., Micropor Mesopor Mater 176 (2013) 162-167

Esterification of LA with primary alcohols

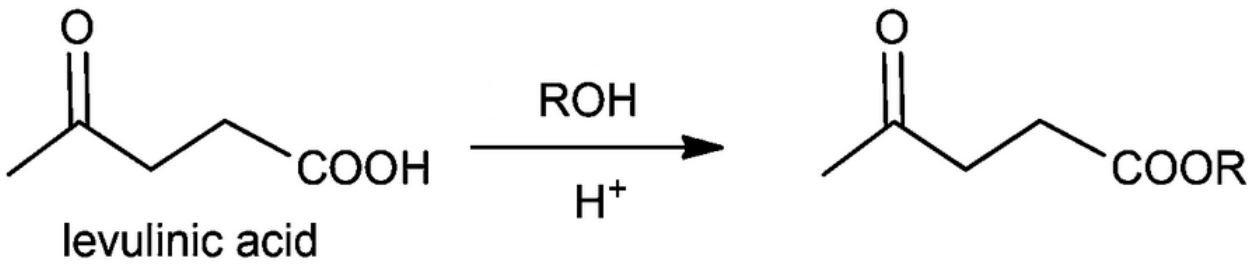

Sulfated metal oxides (solid superacids)

Oxides	Calcination T, oC	Hammett acidity (Ho)
SO_4/SnO_2	550	-18
SO_4/ZrO_2	650	-16.1
SO_4/TiO_2	525	-14.6
SO_4/Al_2O_3	650	-14.6
SO_4/Fe_2O_3	500	-13.0

K. Arata, Green Chem. 11 (2009) 1719-1728.

Acidity: still under investigation!

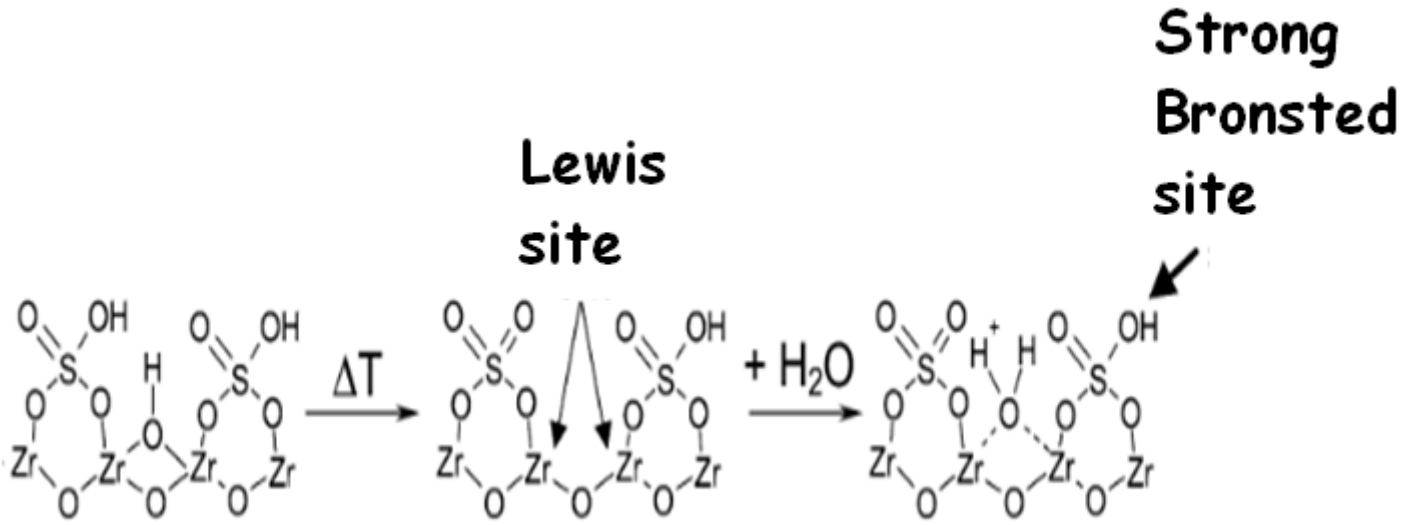

A. Clearfield et al., Catal Today 20 (1994) 295-312

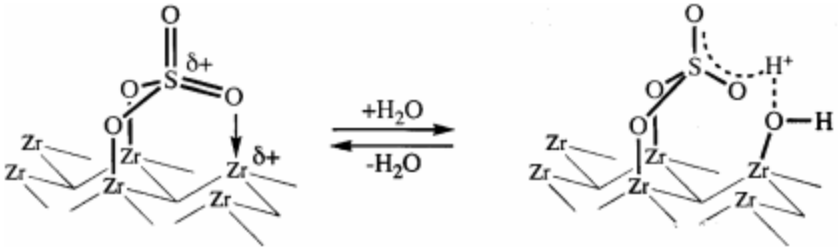

K. Arata, Green Chem. 11 (2009) 1719-1728

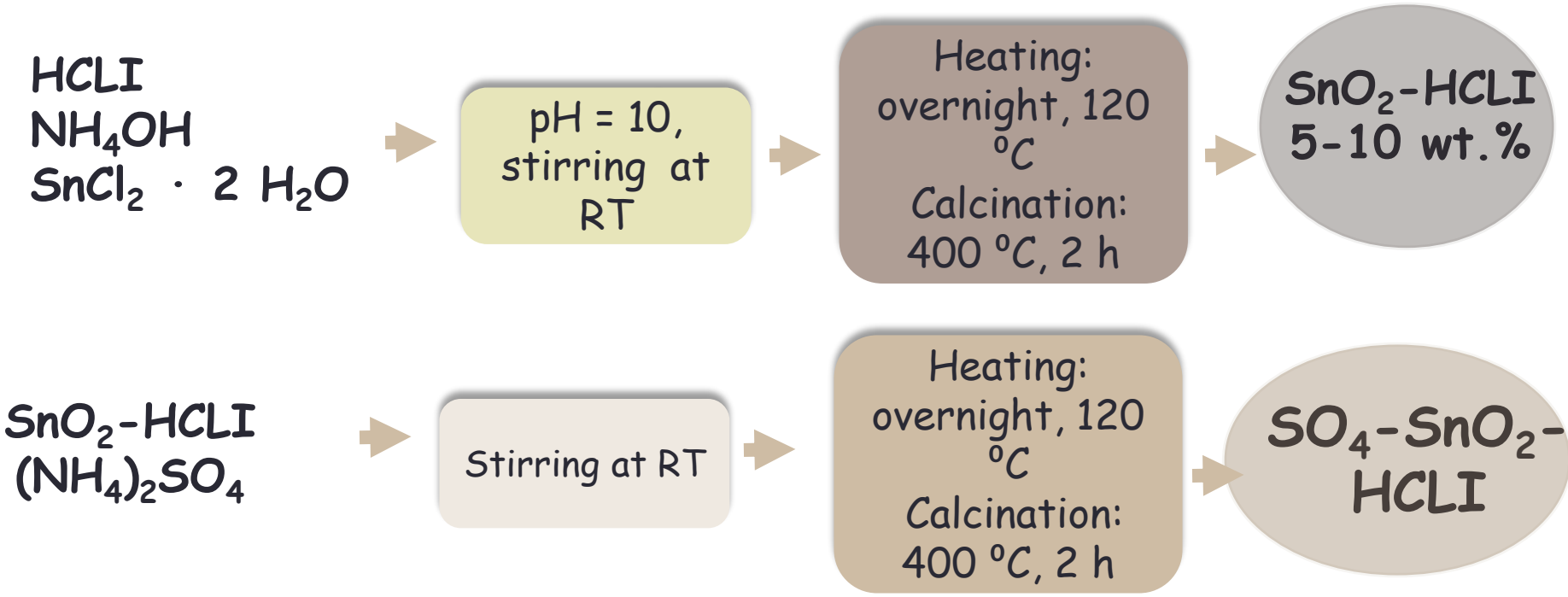
HCLI
NH_4OH
$SnCl_2 \cdot 2\ H_2O$
pH = 10, stirring at RT
Heating: overnight, 120 °C
Calcination: 400 °C, 2 h
SnO_2-HCLI 5-10 wt.%
SnO_2-HCLI
$(NH_4)_2SO_4$
Stirring at RT
Heating: overnight, 120 °C
Calcination: 400 °C, 2 h
SO_4-SnO_2-HCLI

Acidity measurements

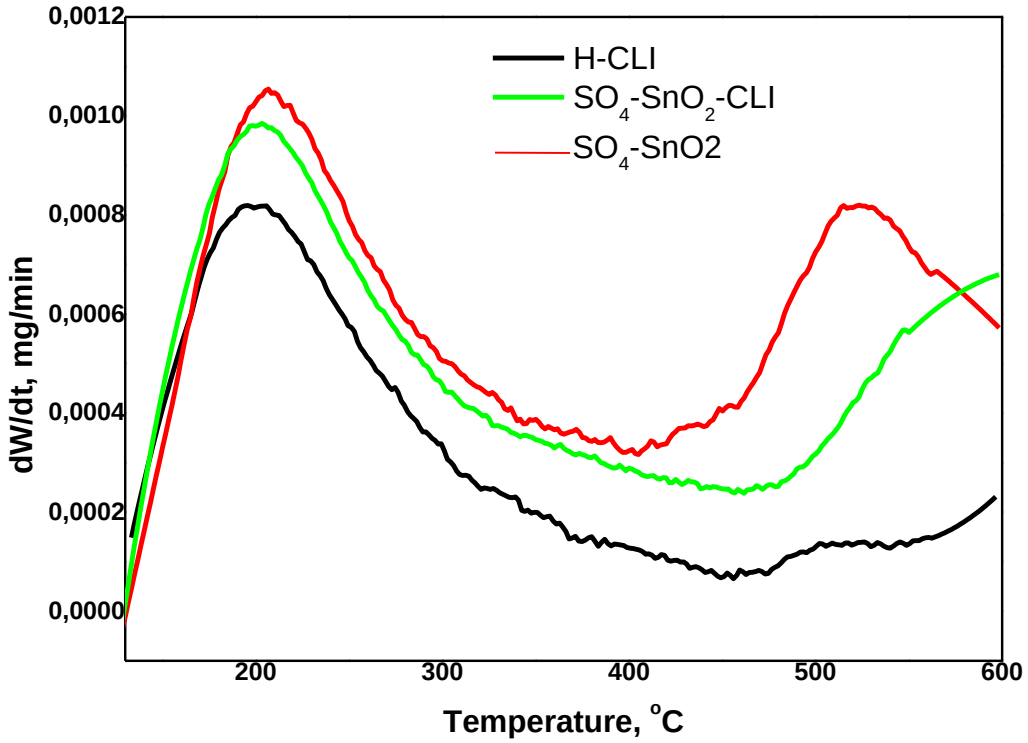

Sample	Acidity, mmol/g
HCLI	0.024
SO_4-SnO_2-CLI	0.141
SO_4-SnO_2	0.302

Catalytic test results

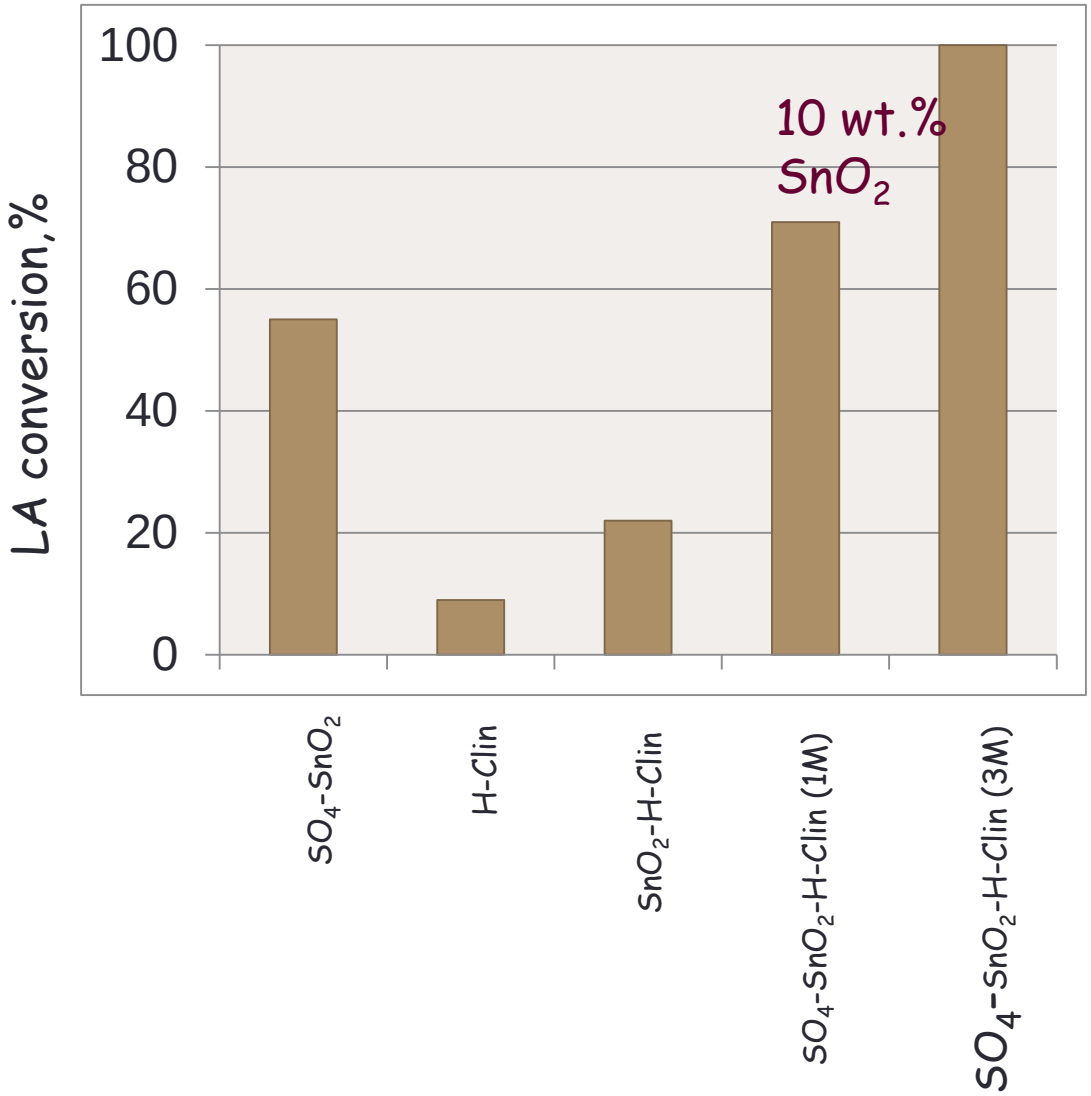

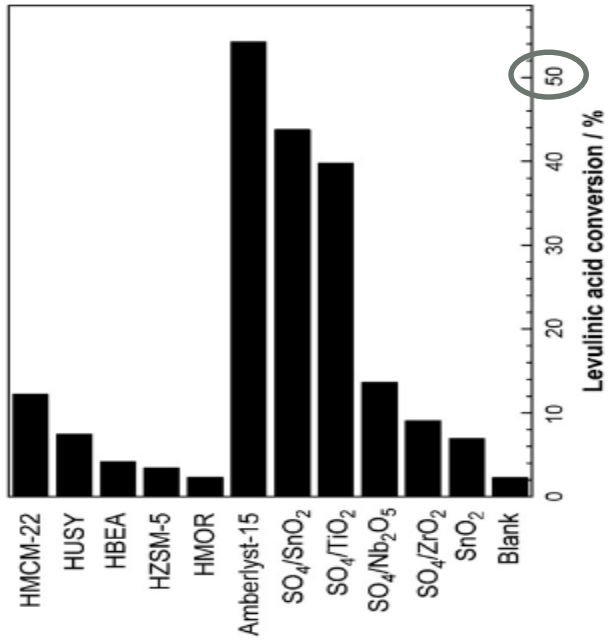

D.R. Fernandes et al., Appl. Catal. A 425-426 (2012) 199-204)

Antimicrobial activity

- Gram- positive:
  - ✓*Staphylococcus aureus*, DSM 799)

- Gram-negative:
  - ✓*Escherichia coli* (DSM 498)

isolates of *E. coli* from the waterborne in Serbia

- ✓*Acinetobacter baumannii* (EU clone I and II)

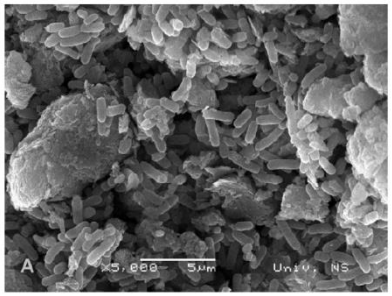

Antibacterial activity against *E. coli* and *S. aureus*

Bacteria	Medium	Cu-Cli		Zn-Cli		Ag-Cli
		Reduction (%) for different time (h)				
		1	24	1	24	1-24 h
E. coli DSM 498	Real effluent	40.1	93.5	8.09	95.1	100
	Synthetic water	19.4	94.9	6.27	93.9	100
S. aureus DSM 799	Real effluent	55.7	86.8	2.79	82.1	100
	Synthetic water	42.8	87.3	3.31	82.3	100

J. Hrenović, et al., J. Hazard Mat 201 (2012) 260-264.

E. coli	Medium	Cu-Z		Zn-Z		Ag-Z
		Reduction (%) for different time (h)				
		1	24	1	24	
Isolate I	Real effluent	73.6	100	40.3	100	100
	Commercial water	84.5	100	82.1	100	
Isolate II	Real effluent	60.2	100	18.0	100	
	Commercial water	64.0	100	26.7	100	

J. Milenkovic et. al, Environ Sci Poll Res (2017), pp. 20273-20281

Antibacterial activity against *A. baumanni* (clinical isolates: European Clone I and Clone II)

Bacteria	Sample	Reduction (%) for different time (h)	
		1	24
EU I	Cu-Cli	100	100
	Zn-Cli	13.0	28.5
	Ag-Cli	100	100
EU II	Cu-Cli	100	100
	Zn-Cli	10.5	22.0
	Ag-Cli	100	100

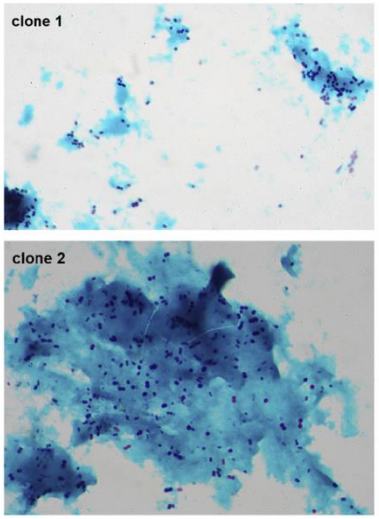

J. Hrenovic et al, Micropor Mesopor Mat 169 (2013) 148-152.

Novel composite: Ag-Cli/PVC with antibacterial action!

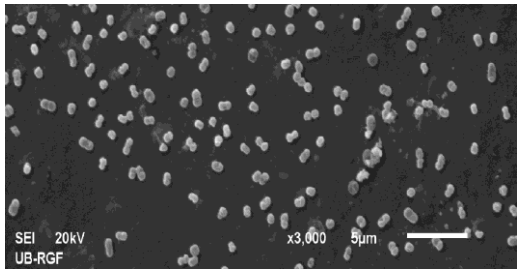

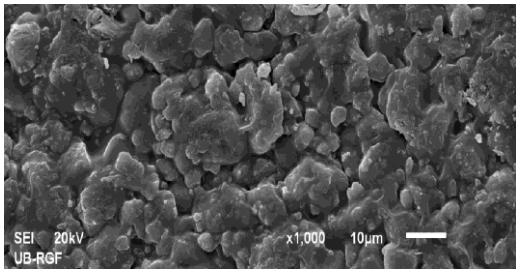

SEM photos of immobilized cells of *A. baumannii* on the surface of the PVC (left) and the absence of bacterial cells on the surface of the composite material (right)

J. Milenkovic et al., Biofouling 30, 965-973 (2014).

Mechanism of bactericidal activity

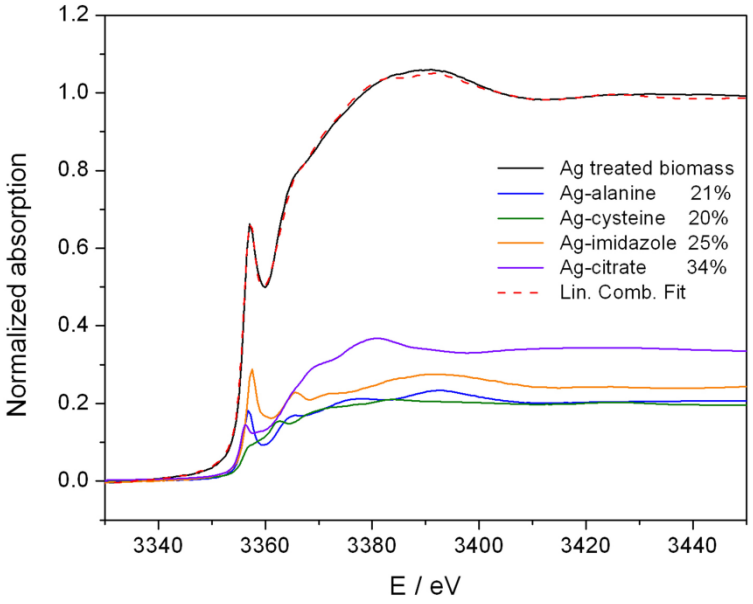

Ag L_3-edge XANES spectrum of Ag-treated *A. baumannii* (solid black line) and the best linear combination fit (dashed red line) obtained by the reference compounds (Ag-alanine, Ag-cysteine, Ag-imidazole and Ag-citrate)

J. Milenković, et al., manuscript in preparation

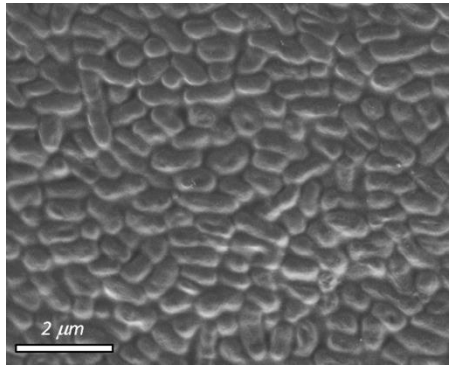

SEM photo of the bacterial sample

Results of XANES:

- Ag bonding to –SH, -NH and –OH

- Ag-N and Ag-O are the dominant binding types

- Antibacterial mechanism might include bonding of Ag ions to the sites in the outer cell membrane of *A. baumannii* as well as to the amino acids or DNA in the cells.

… and other uses

Se-containing zeolitic tuff was tested as soil supplements for the cultivation of *Pleurotus ostreatus* mushrooms.

The fungus adsorb the inorganic Se from zeolitic tuff transforming it to a more useful organically bound form.

S Jevtić et al., Micropor Mesopor Mat 197 (2014) 92-100

This research was supported by the Croatian Science Foundation (grant no. IP-2014-09-5656) under the project title „Natural habitat of clinically important *Acinetobacter baumannii*".

https://www.pmf.unizg.hr/naturaci